

Supporting Information

Metal-free Heptazine-Porphyrin based porous polymeric network as an artificial leaf for carbon-free solar fuels

*Sunil Kumar[#], Venugopala Rao Battula[#], Neha Sharma, Soumadri Samanta, Bhawna Rawat and Kamalakannan Kailasam**

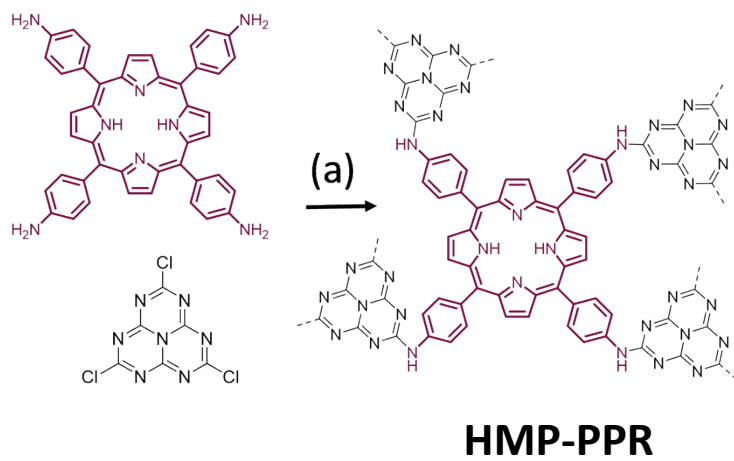
Advanced Functional Nanomaterials, Institute of Nano Science and Technology (INST), Knowledge City, Sector 81, Manauli, SAS Nagar, 140306 Mohali, Punjab, India.

[#] Authors contributed equally

Experimental Section

Synthesis of HMP-PPR:

5,10,15,20-Tetrakis(4-aminophenyl)porphyrin (0.08 g, 0.118 mmol) was taken in a flame dried round bottom flask (RBF-1) and dissolved in 1,4-dioxane (40 ml). Trimethylamine (1 ml) was added and the RBF was stirred for 20 min at room temperature. In RBF-2, trichloroheptazine (0.042 g, 0.153 mmol) was dissolved in 10 ml of dioxane. This solution of RBF-2 was then added to RBF-1 dropwise with constant stirring over the period of 20 min. The reaction mixture was stirred at room temperature for 2 h and then refluxed for 72 h. After that, the reaction mixture was brought to room temperature and then poured over cold water. The precipitates were collected by filtration and washed with dioxane, tetrahydrofuran (THF), methanol and acetone. The precipitates were further purified by soxhlet extraction in THF: methanol (1:1) mixture for 48 h. The precipitates were then collected and dried at 120 °C in the vacuum oven overnight.



Scheme S1. Synthesis route to obtain **HMP-PPR**. (a) trimethylamine, 1,4-dioxane, and reflux for 48 h.

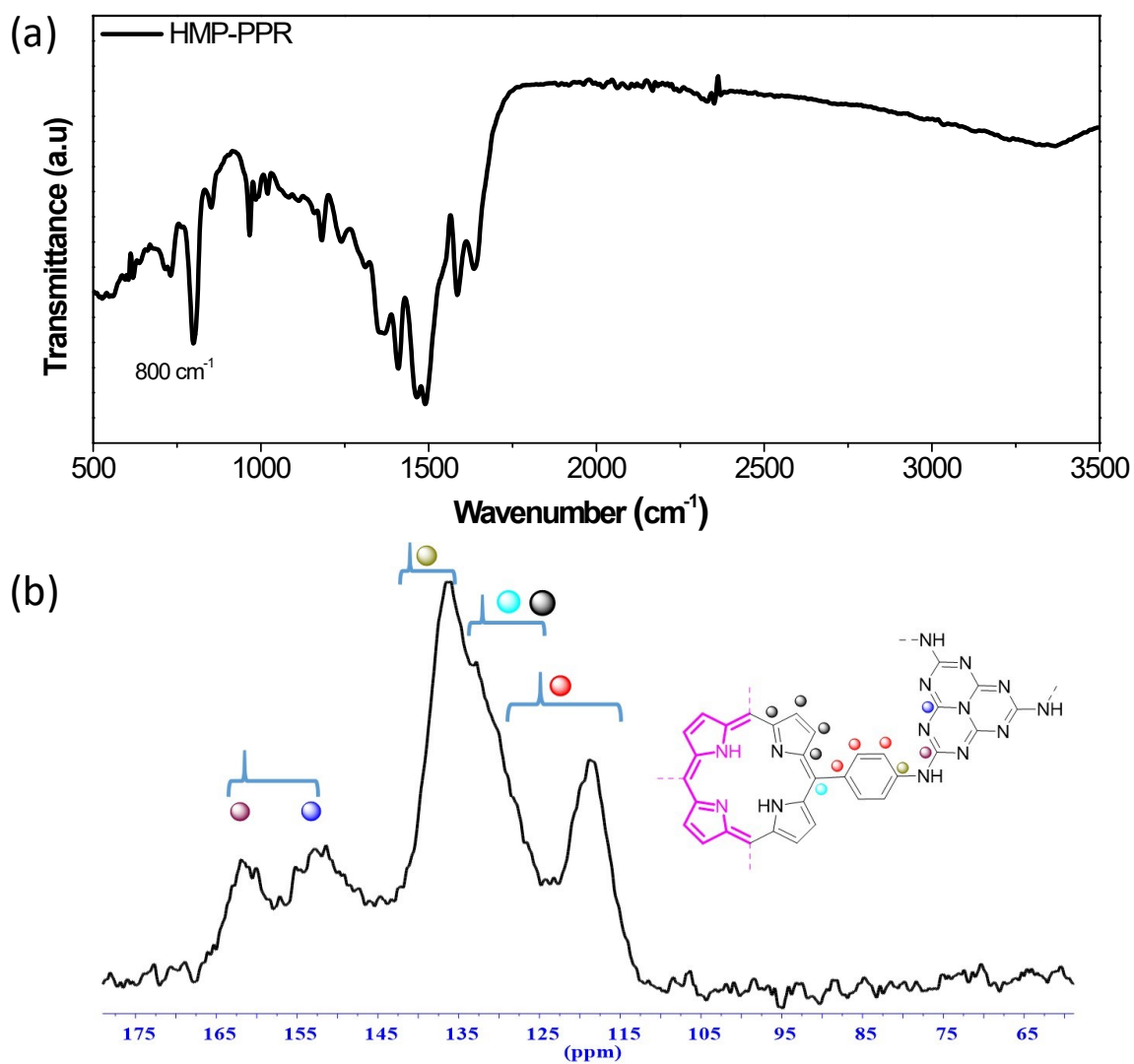


Fig. S1. Structural characterization of HMP-PPR using (a) FTIR and (b) ^{13}C -CP/MAS NMR techniques.

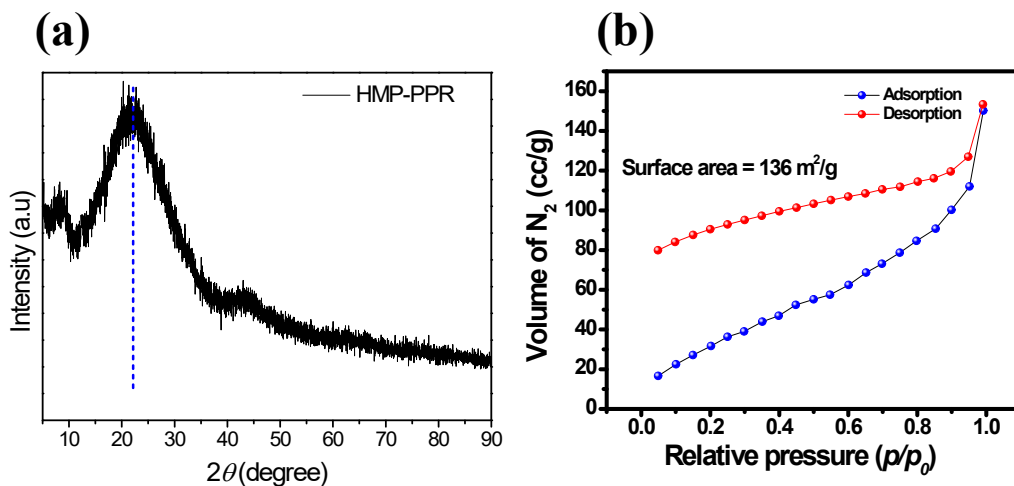


Fig. S2. (a) Powder-XRD and (b) N_2 adsorption-desorption isotherm of HMP-PPR.

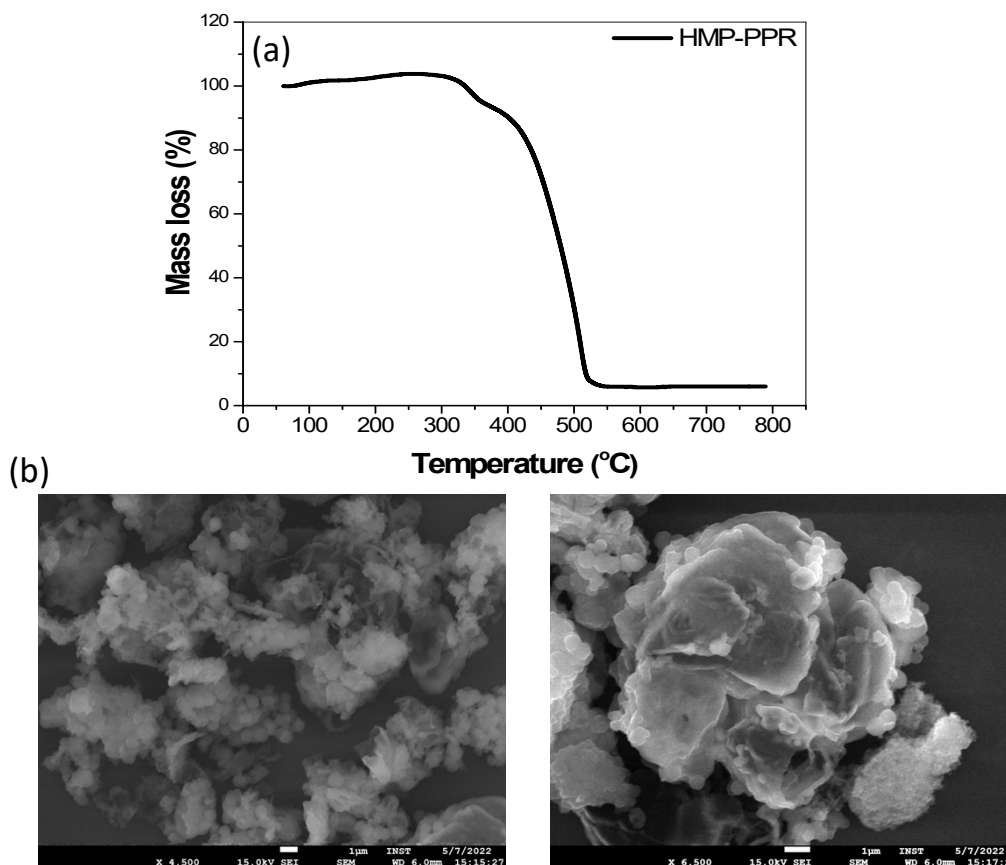


Fig. S3. (a) Thermogravimetric data of HMP-PPR under N_2 atmosphere and (b) SEM images showing the morphology of HMP-PPR.

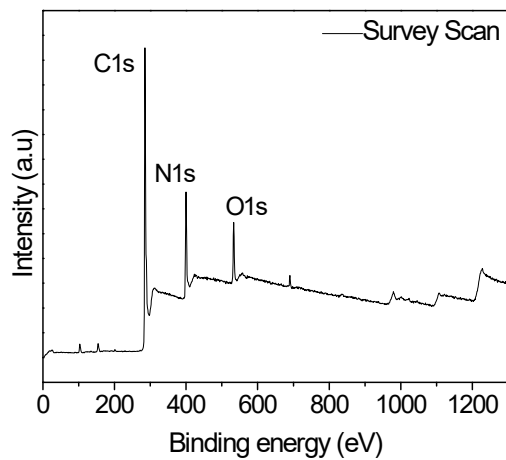


Fig. S4. XPS-survey scan of HMP-PPR.

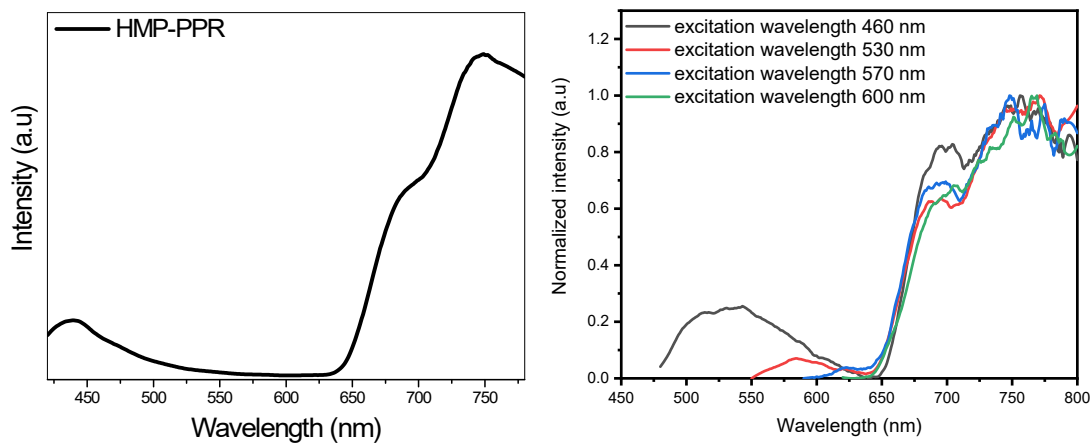


Fig. S5. (a) Photoluminescence spectrum (PL) of HMP-PPR (excitation at 400 nm), and (b) PL data of HMP-PPR at different excitation wavelengths.

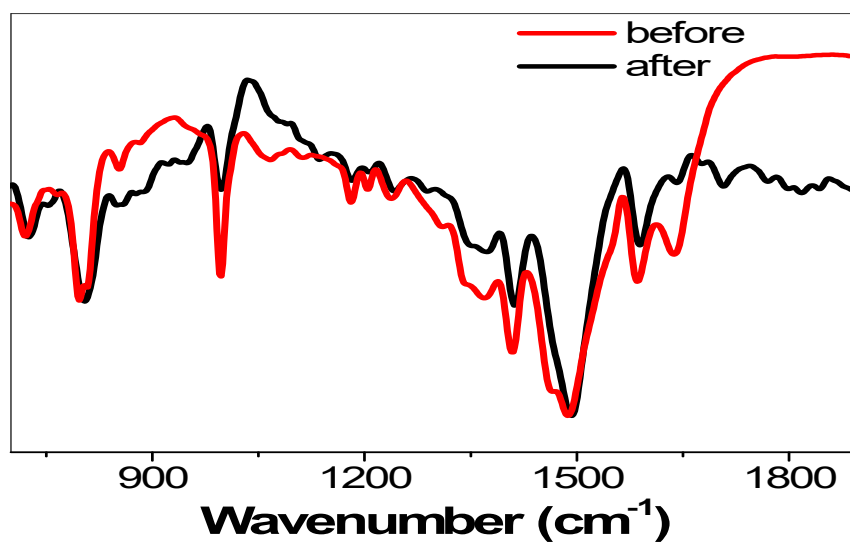


Fig. S6. FTIR spectra of HMP-PPR before and after the photocatalysis.

Photooxygenation of DHN (1,5-dihydroxynaphthalene) to juglone

In order to understand the role of triplet excited states, we have performed the experimental investigation to identify the formation of singlet oxygen studies over HMP-PPR. The photooxygenation of DHN (1,5-dihydroxynaphthalene) to juglone is controlled by the availability of singlet oxygen species ($^1\text{O}_2$) which could be formed by photocatalyst (HMP-PPR in our case) with suitably high triplet state energy. As shown in Figure S9 a and b, the rate of formation of juglone is not matching with rate of decay of 1,5-DHN. These results showed that the singlet oxygen was not produced under these experimental conditions over HMP-PPR. This rule out the possibility of the formation of triplet excited states of HMP-PPR which could transform $^3\text{O}_2$ to $^1\text{O}_2$.

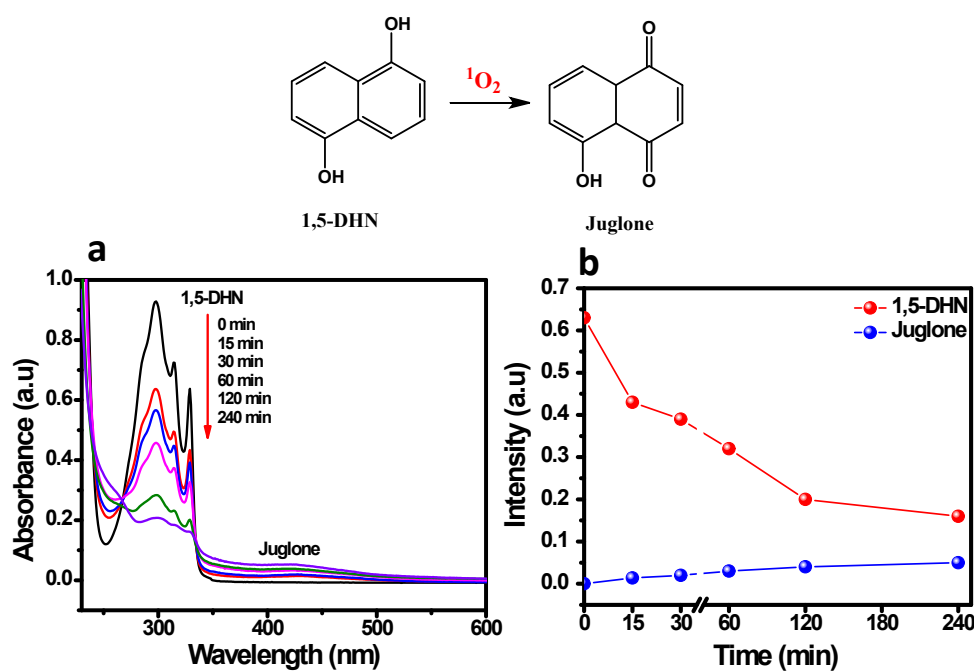


Fig. S7. Photooxidation of 1,5-dihydroxynaphthalene to juglone. (a) Time-dependent absorption spectra of 1,5-DHN under visible light in presence of HMP-PPR. Reaction conditions: 2 mg HMP-PPR, 2 mL IPA and 5 mL ACN, 1 atm O_2 , and $\lambda > 420$ nm. (b) Comparison of decay rate of 1,5-DHN (at 329 nm) and formation rate of juglone (424 nm) in presence of HMP-PPR.

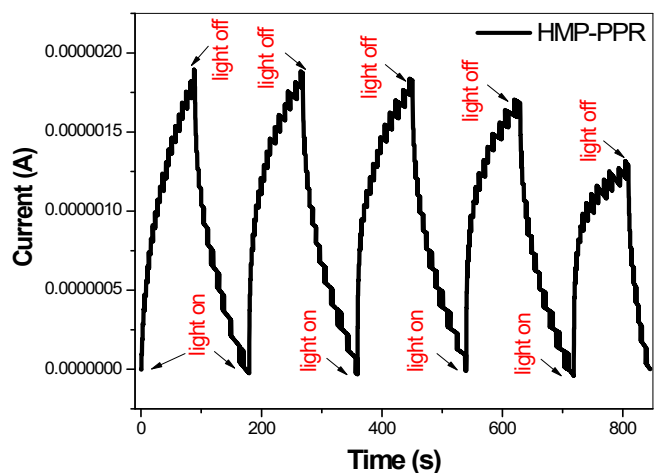


Fig. S8. Photocurrent generation during light on and off cycle.

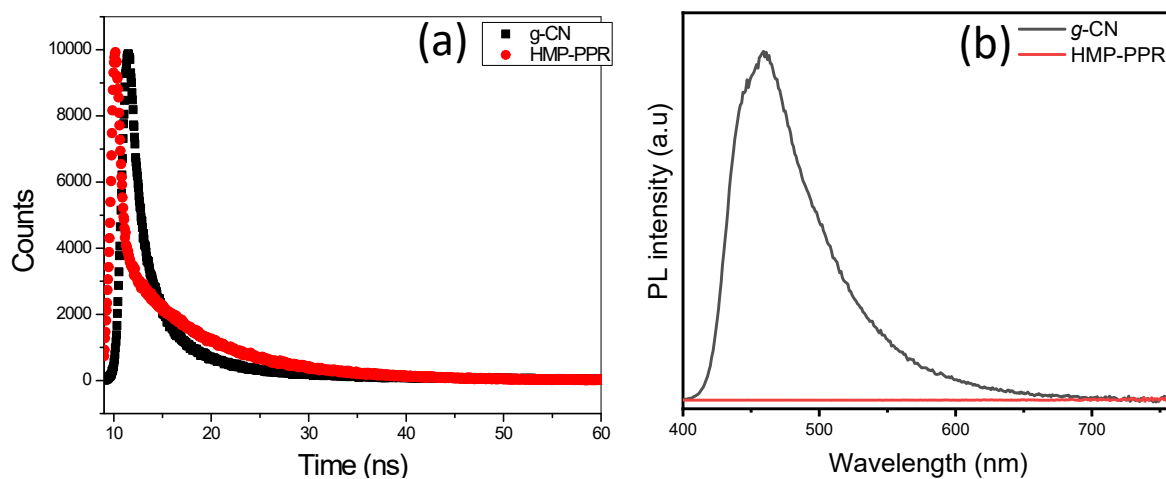


Fig. S9. (a) Lifetime decay curves for HMP-PPR and g-CN, (b) Photoluminescence spectra (PL) of g-CN (excitation wavelength: 390 nm) and HMP-PPR (excitation wavelength 390 nm).

Table S1. Summary of SCC efficiency of g-CN based photocatalysts for solar to H₂O₂ production from water.

S. No	Catalyst	Catalyst	Light source	SCC(%)	Ref
1	HMP-PPR	0.5 g/L	Sun	0.07	<i>This work</i>
2	CO/AQ/C ₃ N ₄	0.5 g/L	AM 1.5G	0.014	1
3	PEI/g-C ₃ N ₄	1 g/L	AM 1.5G	0.045	2
4	Nv-C≡N-CN	1 g/L	AM 1.5G	0.23	3

*SCC = solar to chemical conversion

Table S2. Lifetime data for HMP-PPR and g-CN.

	T1	A1(%)	T2	A2(%)	T3	A3(%)	T4	A4(%)	Avg. Lifetime
HMP-PPR	0.5 2	7	4.03	6	9.14	67	0.06	20	6.5
g-CN	3.1	46	12.7	25	0.08	30	-	-	6.1

References:

1. C. Chu, Q. Zhu, Z. Pan, S. Gupta, D. Huang, Y. Du, S. Weon, Y. Wu, C. Muhich, E. Stavitski, K. Domen and J.-H. Kim, *Proc. Natl. Acad. Sci. U S A*, 2020, **117**, 6376-6382.
2. X. Zeng, Y. Liu, Y. Kang, Q. Li, Y. Xia, Y. Zhu, H. Hou, M. H. Uddin, T. R. Gengenbach, D. Xia, C. Sun, D. T. McCarthy, A. Deletic, J. Yu and X. Zhang, *ACS Catal.*, 2020, **10**, 3697-3706.
3. X. Zhang, P. Ma, C. Wang, L. Gan, X. Chen, P. Zhang, Y. Wang, H. Li, L. Wang, X. Zhou and K. Zheng, *Energy Environ. Sci.*, 2022, **15**, 830-842.